

sorption linewidth for the $1S-2P$ transition be $\Gamma = 1.0 \times 10^2 \gamma$ (or $2.1 \times 10^2 \gamma$). Such a width according to (8) can be provided at the angular radiation aperture $\varphi = 2.2 \times 10^{-3}$ (or 2.1×10^{-3}). Simple evaluations of the saturation intensity of the $1S-2P$ transition within the linewidth Γ in a laboratory frame give the value $I_{s,1} \approx 500 \text{ W/cm}^2$. For a typical pulse duty factor of the proton accelerator 10^{-2} and for a beam diameter of 1 cm the average laser power in the region of λ_1 should be 5 W. From the technical point of view this can be achieved.

Photoionization of excited atoms can be carried out with efficiency approaching 100% in two stages. In the first state, two lasers excite the atoms initially from the $2P$ state into the $3S$ and then into the high-lying Rydberg state nP . When the irradiation angles are chosen correctly, then by virtue of the large magnitude of the Doppler effect, the excitation of atoms on these transitions can be carried out by the lasers in the visible range. If the interaction region is ~ 10 cm, intensities $I_2 \sim 10^2 \text{ W/cm}^2$ and $I_3 \sim 5 \times 10^3 \text{ W/cm}^2$ would be required for the transit time $\sim 0.5 \times 10^{-9}$ sec for the atomic beam in this region. The accelerator duty factor being 10^{-2} , the average powers

will be about 1 and 50 W, respectively. From the technical point of view this is also quite achievable. To ionize atoms from nP state either ir laser radiation or a weak electric field with an intensity of several kilovolts per centimeter which does not change the proton energy, but detaches the loosely bound electron, can be applied.

To conclude we shall note that with this method, by tuning the laser frequency λ_1 we can select any narrow energy interval within the spectrum width of the accelerated protons (transformed into a hydrogen atomic beam). The exact measurement of the wavelength λ_1 provides simultaneously the absolute energy measurement of highly monochromatic protons obtained with accuracy not worse than 10^{-5} .

¹V. S. Letokhov and V. P. Chebotayev, *Nonlinear Laser Spectroscopy* (Springer, Berlin, 1977).

²V. S. Letokhov, V. I. Mishin, and A. A. Puzetzy, in *Progress in Quantum Electronics*, edited by J. Sanders and S. Stenholm (Pergamon, New York, 1977), Vol. 5, Part 3, pp. 139-204.

Search for Six-Quark States

A. S. Carroll, I-H. Chiang, R. A. Johnson, T. F. Kycia, K. K. Ki,
L. S. Littenberg, and M. D. Marx
Brookhaven National Laboratory, Upton, New York 11973

and

R. Cester, R. C. Webb, and M. S. Witherell
Princeton University, Princeton, New Jersey 08540

(Received 26 July 1978)

We have searched the missing-mass spectrum of the reaction $pp \rightarrow K^+K^+X$ for a narrow six-quark resonance in the mass range $2.0-2.5 \text{ GeV}/c^2$. No narrow structure was observed. Upper limits for the production cross section of such a state depend upon mass and vary from 30 to 130 nb.

As the evidence for the colored quark structure of hadrons mounts, the apparent absence of exotic quark combinations becomes more and more puzzling. Nothing in current theory excludes $qq\bar{q}\bar{q}$, six-quark, or even larger states from existing as long as they are color singlets. In recent papers, Jaffe has used the Massachusetts Institute of Technology bag model¹ to calculate the masses of dimeson² and dibaryon³ states. An unexpected prediction emerged from the cal-

culations: There should exist a neutral six-quark, strangeness = -2 state below $\Lambda\Lambda$ threshold that is stable to all but weak decays. Though this result comes from a specific model, Lipkin has argued that the general features of quantum chromodynamics and the known baryon mass splittings imply that the six-quark state with charge zero, spin zero, and strangeness = -2 would have the greatest binding potential.⁴ No prior experiment could exclude the existence of

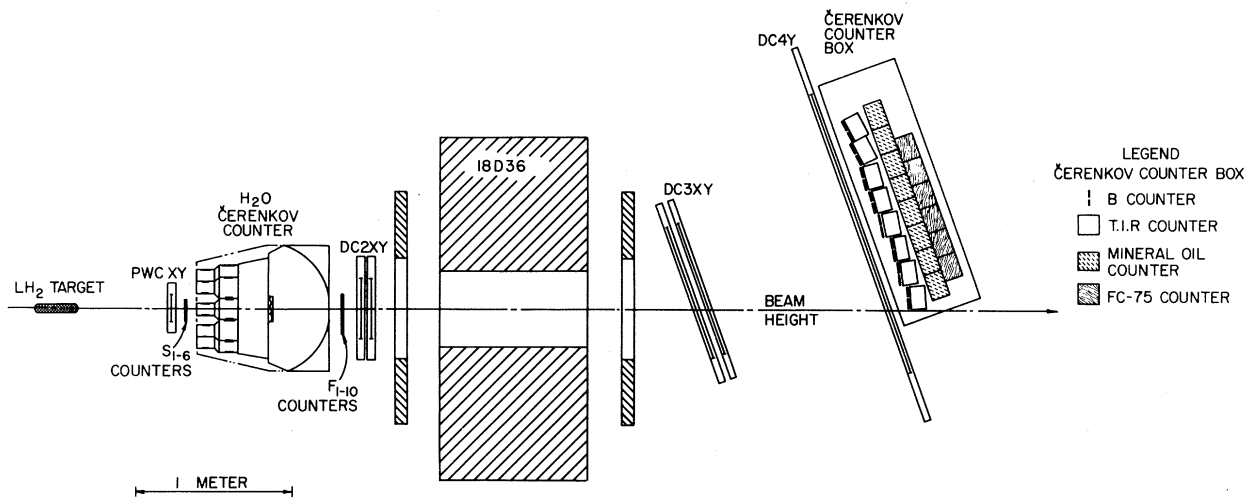


FIG. 1. Elevation view of one arm of the spectrometer. PWC and DC indicate the positions of the proportional wire and drift chambers.

this exotic particle (named the “ H ” by Jaffe) even at the millibarn level.^{5,6}

Last year, an experiment was undertaken at the Brookhaven National Laboratory alternating-gradient synchrotron (AGS) to search for the H in the missing-mass spectrum of $pp \rightarrow K^+K^+X$. This technique not only uniquely defined the baryon number and strangeness of the missing state, but also was insensitive to the decay modes of the state. A double-arm spectrometer with half-angle of 18° , which was used previously in two charmed-particle searches,^{7,8} was modified to improve its kaon-identification ability for particles with momenta from 0.6 to 1.6 GeV/ c . As shown in Fig. 1, each arm was equipped with three hodoscope planes (the S counters measured horizontal position; and the F and B counters, vertical). Between the S and F counters was a water differential Čerenkov counter which was used for pion identification. Proportional wire and drift chambers were used to measure particle trajectories and momenta. Behind the last set of drift chambers were three sets of Čerenkov counters. The first set of counters consisted of Lucite blocks wrapped in black paper. Photomultipliers at one end of the blocks detected only the Čerenkov light produced at angles greater than that for total internal reflection. The effective kaon threshold in these counters was 1.0 GeV/ c . The orientation of each of these counters was chosen to maximize the proton-kaon discrimination for particles with momenta less than 1.6 GeV/ c . The total-internal-reflection counters were followed by a set of threshold Čerenkov

counters filled with mineral oil. The final set consisted of threshold counters filled with FC-75. The effective kaon thresholds were 0.55 GeV/ c for the mineral oil and 0.8 GeV/ c for the FC-75 counters.

Events were selected with a two-step trigger system. A fast trigger was generated by a coincidence of pulses from the S , F , and B counters in both arms and no pulse in either water Čerenkov counter. This trigger initiated the readout system, which recorded the chamber coordinates, the pulse-height and timing information from the hodoscopes, and the pulse heights of all Čerenkov counters. Simultaneously with the beginning of the readout cycle, a set of six coincidence matrices estimated the momenta of the particles in each arm from the F - and B -counter hits, and then determined if the appropriate bank of Čerenkov counters had fired. If so, the event was written on tape; if not, the event was quickly cleared and the readout system reset.

The small acceptance of the apparatus (geometric and momentum acceptance covered approximately 0.01% of the phase space), the need for good missing-mass resolution, and the desirability of probing into the nanobarn range of cross sections mandated a high-intensity monoenergetic proton beam free of K^+ and π^+ contamination. To provide this, the AGS was operated at approximately 5 GeV/ c for this experiment. The internal protons were extracted by diffractive Coulomb scattering and transported through the normal SEB channel to a 9-in. liquid hydrogen target. The spill length from the AGS was increased to

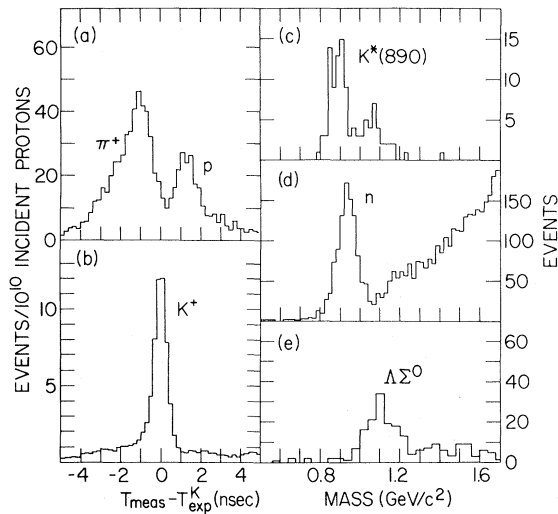


FIG. 2. (a) Time-of-flight distribution for all two-particle coincidences (without water-Čerenkov-counter veto) relative to the expected time of flight for a kaon. (b) The same time-of-flight distribution as (a) except with full trigger logic and off-line Čerenkov-counter cuts. (c) Effective mass of $K^+\pi^-$ system from $pp \rightarrow K^+\pi^-X$. Data are from two special runs in which the polarity of one arm was reversed. (d) Missing mass recoiling against $p\pi^+$ system in $pp \rightarrow p\pi X$ at 5.3 GeV/c. Data are from $L \cdot R$ calibration runs. (e) Missing mass recoiling against pK^+ system in $pp \rightarrow pK^+X$ at 5.3 GeV/c. Data are from a " Λ " trigger which required a K^+ in one arm and a high-momentum particle in the other.

7 sec to achieve better utilization of the accelerated beam while staying within the intensity limitations of the apparatus. Typically the experiment ran with intensities of 3×10^8 protons/sec with duty factors in excess of 75%.⁹ The beam momentum was determined by measuring the frequency of the AGS accelerating voltage. Data were collected at three different incident beam momenta: 5.1, 5.4, and 5.9 GeV/c.

Off line, particles were identified from the Čerenkov-counter pulse heights and from S-, F-, and B-counter timing information. The time-of-flight distribution of all particles satisfying the left-right coincidence circuitry (without momentum logic or water-Čerenkov-counter veto) is illustrated in Fig. 2(a). No kaon signal is apparent between the pion and proton peaks. Figure 2(b) shows the distribution when the full trigger logic and the off-line Čerenkov-counter cuts are applied. The observed kaon timing signal has a resolution of $\sigma = 0.32$ nsec.¹⁰

Calibration runs with special triggers were taken periodically. One type of these runs mea-

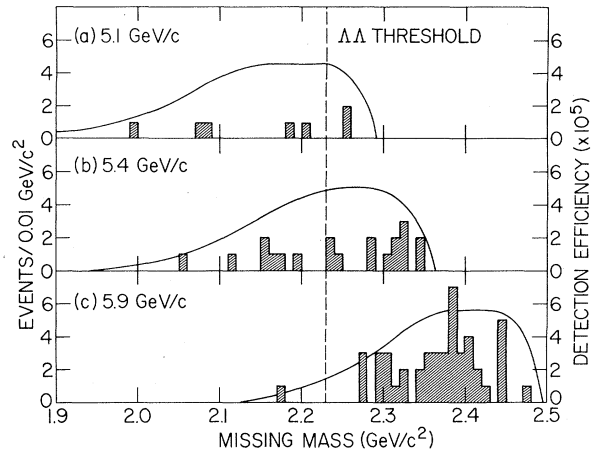


FIG. 3. Missing mass recoiling against K^+K^+ system in $pp \rightarrow K^+K^+X$. The slashed boxes are the actual observed events; the solid line, the detection efficiency as a function of mass. The detection efficiency was determined by a Monte Carlo program which generated events flat in three-particle phase space.

sured the $K^*(890)$ inclusive production in the reaction $pp \rightarrow K^+\pi^-X$; another measured the cross section for $pp \rightarrow p\pi^+n$; and a third, Λ and Σ^0 production in $pp \rightarrow pK^+X$. Mass plots for these three reactions are displayed in Fig. 2(c)–2(e). After corrections for geometric acceptance, particle-identification biases, and kaon decay, the observed cross sections for these three reactions were consistent with cross sections inferred from earlier measurements.^{11–13} We were also able to verify the field integral of the spectrometer magnets, the beam momenta, and the missing-mass resolution from these runs.

The missing-mass spectrum for the reaction $pp \rightarrow K^+K^+X$ at each of the three incident beam momenta is shown in Fig. 3. The mass-dependent detection efficiency for phase-space production is also given.¹⁴ Missing-mass resolution is limited by multiple scattering in the water Čerenkov counter and the target,¹⁵ and has a rms width $\sigma = 6$ MeV/ c^2 . As can be seen in Fig. 3, no obvious narrow structure is observed between 2.0 and 2.5 GeV/ c^2 . Events below $\Lambda\Lambda$ threshold can come from three sources (other than exotic-particle production): πK or pK events misidentified as KK events, KK accidental coincidence, or double-scattering events such as $pp \rightarrow K^+p\Lambda$ where either the p or the Λ interacts again to give a second kaon. Misidentification of pions and protons (the major source of background) occurred most often for high-momentum particles. Consequently,

TABLE I. 90%-confidence-level (90% C.L.) upper limits for the production cross section (in nanobarns) of narrow dihyperon resonance.

Beam momentum (GeV/c)	Mass interval (GeV/c ²)	90% C.L. upper limits (nb)
5.1	2.0-2.1	130
5.1	2.1-2.23	50
5.4	2.1-2.23	40
5.4	2.23-2.35	30
5.9	2.23-2.35	130
5.9	2.35-2.48	90

background events are expected to congregate in the lower half of the missing-mass plots. In fact, the number of events observed below $\Lambda\Lambda$ threshold is consistent with the number expected from the background sources, while only about 20% of the above threshold events come from these sources. The events observed above threshold in Figs. 3(b) and 3(c) correspond to an average cross section (assuming that production is flat in phase space) of $d\sigma/dm = 0.18 \pm 0.07 \mu\text{b}/(\text{GeV}/c^2)$ at 5.4 GeV/c and $1.2 \pm 0.3 \mu\text{b}/(\text{GeV}/c^2)$ at 5.9 GeV/c. The upper limits for the production cross section of a narrow strangeness = -2, dibaryon resonance are given in Table I. These limits are orders of magnitude below previous work and slightly below phenomenological estimates made from the measured $\Lambda\Lambda$ production rate.¹⁶ Nevertheless, in the absence of more reliable estimates of the production cross section, the possibility of the existence of the H cannot be excluded.

We would like to thank the Accelerator Department staff for their cooperation operating the accelerator in this unusual mode. J. W. Glenn, III, deserves special thanks for his efforts in setting up and maintaining the high duty cycle for the proton extraction. We also appreciated the support and encouragement provided by Professor V. L. Fitch.

This work was supported by the U. S. Department of Energy under Contracts No. EY 76-C-02-0016 and No. EY 76-C-02-3072.

¹T. DeGrand *et al.*, Phys. Rev. D **12**, 2060 (1975).

²R. L. Jaffe, Phys. Rev. D **15**, 267 (1977).

³R. L. Jaffe, Phys. Rev. Lett. **38**, 195, 617 (1977).

⁴H. J. Lipkin, in *Prospects for Strong Interactions at Isabelle*, edited by D. P. Sidhu and T. L. Trueman (Brookhaven National Laboratory, Upton, N. Y., 1977).

⁵Bubble-chamber experiments such as those by G. Wilquet *et al.*, Phys. Lett. **57B**, 97 (1975), and by W. Chinowsky *et al.*, Phys. Rev. **165**, 1446 (1968), have inherent scanning and reconstruction biases against finding this state. Double-arm counter experiments have not been performed.

⁶There exists some evidence against the existence of the H with mass less than 11 MeV/c² below $\Lambda\Lambda$ threshold from hypernuclear emulsion observations. See, for example, D. J. Prowse, Phys. Rev. Lett. **17**, 782 (1966), and M. Danysz, Nucl. Phys. **49**, 121 (1963).

⁷R. Cester *et al.*, Phys. Rev. Lett. **37**, 1178 (1976).

⁸R. Cester *et al.*, Phys. Rev. Lett. **40**, 139 (1978).

⁹A. S. Carroll and J. W. Glenn, Brookhaven National Laboratory, Accelerator Department, Experimental Planning and Support Division, Informal Report No. 78-2 (unpublished).

¹⁰The timing difference between the left and right arm had comparable resolution; a cut on this parameter eliminated much of the accidental background.

¹¹The K^* acceptance of the experiment covered a small region of phase space centered at $y_{c.m.}^* = 0.18$ and $p_T = 0.15 \text{ GeV}/c$. The measured invariant cross section for K^* production at 5.9 GeV/c is $E d^3\sigma/dp^3 = 50 \pm 10 \mu\text{b}/\text{GeV}^2$. For comparison, the result of V. Blobel *et al.* [Phys. Lett. **48B**, 73 (1974)] in the same $y_{c.m.}^*$ and p_\perp region interpolates to 200 and 330 $\mu\text{b}/\text{GeV}^2$ for proton beams of 12 and 24 GeV/c, respectively.

¹²G. Alexander *et al.*, Phys. Rev. **154**, 1284 (1967).

¹³W. Chinowsky *et al.*, Phys. Rev. **165**, 1446 (1968).

¹⁴The product of reconstruction and trigger efficiencies was approximately 10%, although it varied slightly from momentum to momentum. The effective fluxes represented in Fig. 3 are 2.0, 5.4, and 2.1×10^{12} protons for the 5.1-, 5.4-, and 5.9-GeV/c data, respectively.

¹⁵The particles detected in the calibration reactions $pp \rightarrow K^*X$, $pp \rightarrow p\pi n$, and $pp \rightarrow pK^+\Lambda$ are in a different region of phase space where the momentum measurements dominate the mass resolution. The observed width of these peaks are consistent with our expected resolutions.

¹⁶Just above threshold $\sigma(pp \rightarrow \pi^+\pi^0 d)/\sigma(pp \rightarrow \pi^+\pi^0 pn) \approx 0.2$. If $\sigma(pp \rightarrow K^+K^+H)/\sigma(pp \rightarrow K^+K^+\Lambda\Lambda)$ is similar, the H -production cross section at 5.9 GeV/c would be 90 nb.